# Spray resulting from High Pressure Atomization with low L over D Multihole Injectors and the role of the Cavitation

S. Makhlouf[1]*, J. Hélie*, O. Grimoux*, J. Cousin**, L. Gestri+, A. Wood++, G. Wigley++.
samir.makhlouf@continental-corporation.com
*Continental Automotive SAS, Toulouse, France
** CORIA laboratory, Rouen, France
+ Continental Automotive, Pisa, Italy
++ Loughborough University, England.

**Abstract**

Two different low L/D nozzle designs are tested: one version with a sharp entrance (normal injector) and a second version submitted to hydro-grinding to smooth out the nozzle entrance rounding radius in order to counteract the cavitation trend. The resulting spray is analyzed in a close view by direct imaging shadowgraphy and by PDA (Phase Doppler Anemometry).

The comparisons presented, due to the reduction in cavitation on one side of the nozzle in the hydro-ground injector, show that the overall spray morphology is different in comparison to the normal injector. Asymmetric cavitation causes the spray, especially its dense region, to tend towards the injector axis. As the cavitation at nozzle exit is reduced, the angle of the dense spray region is increased and the spray width is reduced.

Having cavitation on one side of the nozzle changes the velocity field of the flow, hence the jet experiences a transverse motion. Further analysis shows that at high pressures the mixing of hydro-ground injector's spray takes place further downstream than for the normal injector. PDA results also do agree with these findings, showing increased droplet axial velocity for the hydro-ground injector, and also a reduction in the range of droplet flow angles, which results from the reduced levels of cavitation. Therefore, cavitation inside the nozzle improves the dispersion of the spray because as soon as the bubbles emerge from the nozzle they break the liquid structures and increase the injection angle. Droplet sizing was applied and surprisingly both sprays lead to close droplet diameters; which means that the result of the overall atomization process is not dramatically influenced by cavitation. These features behaviours are discussed in the paper by analyzing the resulting sprays from the two injectors.

## 1- Introduction:

The present generation of High Pressure Gasoline Direct Injection multihole atomizers are characterized by a short hole of length (L) over diameter (D) around unity. This makes the distinction with the diesel HPDI atomizers. This experimental work continues what it is studied in a twin paper from CORIA [1] at a low injection pressure with sub-atmospheric back pressure and is complementary to the previous simulation efforts made by Khan et al. [2] and Shi et al. [3]. In this previous work the role of the coherent structures in the nozzle liquid flow has been investigated at low pressure. Here, at higher pressure, due to the viscosity and the vapour pressure, the liquid flow is submitted to cavitation just before exiting.

The purpose of this study is to understand the effect of cavitation in the injector nozzle on the resulting spray. Cavitation is generated at the inlet of nozzle orifice where the change in cross-section and flow direction takes place. Chaves [4] showed the influence of changing the nozzle geometry on the cavitation development which is most sensitive to the local inlet geometry of the orifice and to the flow conditions at this point. The r/D ratio, in which r is the rounded radius and D is the exit diameter of nozzle orifice, is the relevant factor controlling geometric cavitation [4, 5]. This paper presents the results collected from the measurements of two XL2 injectors on a close-up test bench and on a PDA test bench as well. The measurements were conducted at three different injection pressures: 5, 60 and 130 bar. One of the injectors is a standard Continental serial XL2 while the second one is modified. Aiming to reduce cavitation, the second injector has a rounded nozzle inlet which is made by hydro grinding process [6].

### *1.1 Experimental set-up of close-up test bench:*

Spray images are captured by a Fuji S5 Pro CCD camera - the field of view is 24*36 mm - recording shot to shot images with a resolution set to 2 µm/pixel. The illumination lamp is a nanolite with around 20 mJ of energy at each pulse, controlled by a driver, and aligned on the optical axis of the camera. Its flash duration is about 11ns, which is short enough to avoid image blurring. The injector is fixed in between by precise NewPort micrometrics actuation and a lens focuses the light beam on the injector tip. The fuel used is N-heptane and is injected into ambient conditions (temperature ~18°C). A hydraulic system feeds the fuel from the tank to the

[1] Corresponding author: samir.makhlouf@continental-corporation.com

injector. The pump speed is controlled with a computer and the injection pressure is measured by a transducer. The injection event is controlled by a SDI drivebox Continental. All parts are connected and synchronized thanks to a National Instrument card. Commands are given from the computer using LabView software programmed by Assystem Company. The camera is equipped by 3 sets of 3 rings each and a 105 mm objective to reach a magnification of 5.5. Finally, pictures are taken after 2 ms from the injector's needle opening command; hence the quasi-steady conditions are reached.

### *1.2 Experimental set-up of PDA test bench:*

The design, construction and application of the Loughborough University two component PDA transmission system to study dense GDI fuel sprays has been well documented [7]. The configuration for the 488 and 514 nm laser beam wavelengths at the final focusing lens was: beam diameters of 5 mm, equal beam pair separations of 50 mm, laser powers of 100 and 200 milli-watts per beam with a horizontal polarisation. With a focal length lens of 300 mm this produced coincident measurement volumes of diameters of 37 and 39 microns with fringe spacings of 2.94 and 3.10 microns respectively for the two wavelengths. The 514 nm beam pair was in the vertical plane to measure the axial droplet velocity and size with the 488 nm beam pair in the orthogonal plane to measure the radial droplet velocity.

The Dantec 57X10 receiver was positioned at a scattering angle of 70 degrees with the polariser set to collect only scattered light in the horizontal plane and an aperture micrometer setting of 0.5 mm. This optical configuration resulted in an effective measurement volume length of 0.1 mm. In-conjunction with the Dantec processor the transmitter and receiver set up produced a droplet velocity bandwidth of -30 to 110 m/s with a drop size measurement range up to 100 microns.

The three-hole GDI injector was supported from a gantry incorporating a rotation stage and three precision orthogonal linear traverses to orientate and position the spray in three dimensions relative to the static PDA measurement volume. Each radial scan started from the geometric vertical axis through the nozzle tip and traversed out to the periphery of the spray stream. The measurement co-ordinates in the vertical plane were Z = 10, 20, 30, 40, 50 and 60 mm below the nozzle tip. The horizontal traverse was computer controlled and programmed with a radial step increment of nominally 7 - 10% of the Z value in order to resolve local high velocity gradients across the cone of the spray stream in the horizontal plane.

### *1.3 Geometrical basics of XL2:*

The XL2 nozzle is characterized by L/D ratio close to 1. The diameter of the nozzle D is 0.194 mm. Its mass flow rate is equal to 5.92 g/s at 100 bar injection pressure. The geometrical direction of the nozzle makes an angle of 23° (shorter arrow in fig.1) with the vertical position of the injector. Unfortunately the XL2 injector tip design has a "negative" aspect in respect to what could be seen of close-up bench images using diesel protruded tip for example. This geometrical aspect makes us lose the upper part of the spray. From the exit of the nozzle until 0.82 mm downstream, the spray cannot be photographed. Given that we photograph a sloping jet, and that we square 5 mm underneath the injector, it means that we are capturing the part between 1 mm and 6 mm away from the nozzle orifice. At those distances near the nozzle exit the liquid jet atomization depends on cavitation regime [8]. Image square in figure 1 shows the mean spray of 200 shot to shot images. The longer arrow (fig.1) is the mean direction of the dense spray part (darkest part in fig.1), it will be determined in section 2. The other arrow is the geometrical nozzle direction. In our case, the angled nozzle creates an asymmetric location of cavitation [4]. The main effect should be on the right side of the nozzle where the inlet corner involves the larger deflection of the flow [4, 9] coming from the external sealing bond side. We name the sealing bond, which is on the right side of the circled area in fig.1, as the external side. On the opposite side of this area is the central injector body axis. Furthermore, Ganippa et al. [10, 11] concluded – at least at moderate fuel pressure (but Re between 50,000 and 100,000) – that the asymmetric distribution of cavitation within the hole and its extension to nozzle exit produce a jet that is atomizing on the side where cavitation is present and non-atomizing on the other side where there is less cavitation.

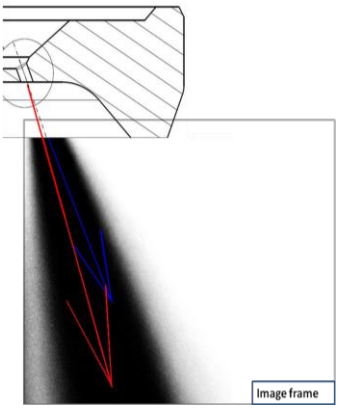


**Figure 1 : XL2 injector geometry and image frame of the spray.**

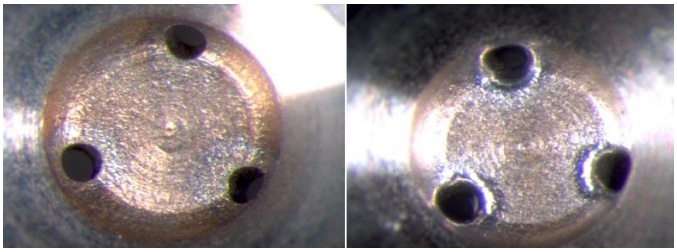

**Figure 2: two different nozzle designs photographed from the sac side (hydro on the right).**

Figure 2 shows two images taken from the injector sac side that compare the nozzle inlet with the normal injector, on the left, and the hydro-ground injector on the right. The entrance of the normal injector nozzle is a sharp edged one. In the other injector, nozzle seats have a rounded shape. The rounded inlet thickness is approximately 0.053 mm, which gives an r/D ratio close to 0.27.

**2- Effect on the mean direction and jet angle:**

The images taken from the close-up test bench are put through a post treatment process where they are transformed from RGB to a grey scale image using the green frame. The background is subtracted from each image. The resulting images are summed and normalized to give the mean image which is also a grey image. The pixels that have the extreme value of 1 are the pixels where all the 200 sprays went through. In contrary the pixels that have the extreme value of 0 are those where none of the sprays went through. Therefore, this final image contains the probability $P_{i,j}$ (from 0 to 1) of how many sprays went through pixel (i,j). Obviously, the probability concerns the shadowgraphy – i.e. an integral light absorption submitted to biased optical effect and saturation – and not directly the spray density itself. However, as shadowgraphy has been frequently applied for decades on spray visualization it is assumed to be a mostly representative measure of the spray feature.

***2.1 Jet mean direction:***

The jet mean direction is given by the equation:

$$\overline{\beta} = \frac{\sum_{i,j} \beta_{i,j} \cdot P_{i,j}}{\sum_{i,j} P_{i,j}},$$

Where $\beta_{i,j}$ is the angle between the vertical line of mean image and the line made by pixel (i,j) with the centre of nozzle exit area. Thus, $\overline{\beta}$ is the angle that separates the jet mean direction from the vertical line. Once the jet mean direction angle is found, a standard deviation can be calculated for each side of the mean jet using the equation below:

$$\text{std} = \sqrt{\frac{\sum_{i,j} (\beta_{i,j} - \overline{\beta})^2 \cdot P_{i,j}}{\sum_{i,j} P_{i,j}}}.$$

When the only pixels taken into consideration are those of the external side – the term in brackets is positive – then the result is the external side standard deviation. Otherwise the result is the central side standard deviation of $\beta$. Results are presented in table 1.

***2.2 Dense spray mean direction:***

The mean grey image of 200 shot to shot images needs to be binarized so we only keep the dense spray part. This means that we need to apply a binarization program to define an adequate threshold. Once the threshold is fixed, the same post treatment is applied on the mean image of "x" shot to shot images. The variable "x" goes from 1 to 200, and this loop proves that the average value of the dense spray mean direction angle is independent of the number of images after a certain "x" value. This procedure is done for all the studied cases here and the threshold values (binarization level) are also listed in table 1.

***2.3 Angle results and discussions:***

With the XL2 normal injector case, the jet is the most inclined toward the injector centre axis (see table below) because it has the smallest angles of jet mean direction and dense spray mean direction (fig.3 left side graph). The difference in angle between the spray mean direction and the dense spray direction is much more pronounced in the normal injector case. The reason could be that recirculating bubble on the external edge of the nozzle is forcing the flow to direct toward the central side, as well as the resulting spray, especially its dense part.

| XL2 design | $\overline{\beta}$ (°) | Exterior std (°) | Central std (°) | Dense spray (°) | Pressure (bar) | Binarization level |
|---|---|---|---|---|---|---|
| Normal | 19.174 | 9.785 | 8.382 | 15.21 | 5 | 0.2 |
| Hydro | 21.63 | 8.92 | 8.577 | 19.9 | 5 | 0.2 |
| Normal | 17.1 | 13.432 | 11.35 | 16.98 | 60 | 0.35 |
| Hydro | 19.256 | 9.876 | 10.424 | 19.33 | 60 | 0.35 |
| Normal | 17.513 | 11.41 | 10.78 | 16.16 | 130 | 0.4 |
| Hydro | 19.04 | 10.385 | 10.51 | 18.99 | 130 | 0.4 |

**Table 1: Angle values for both XL2 designs at 5, 60 and 130 bar.**

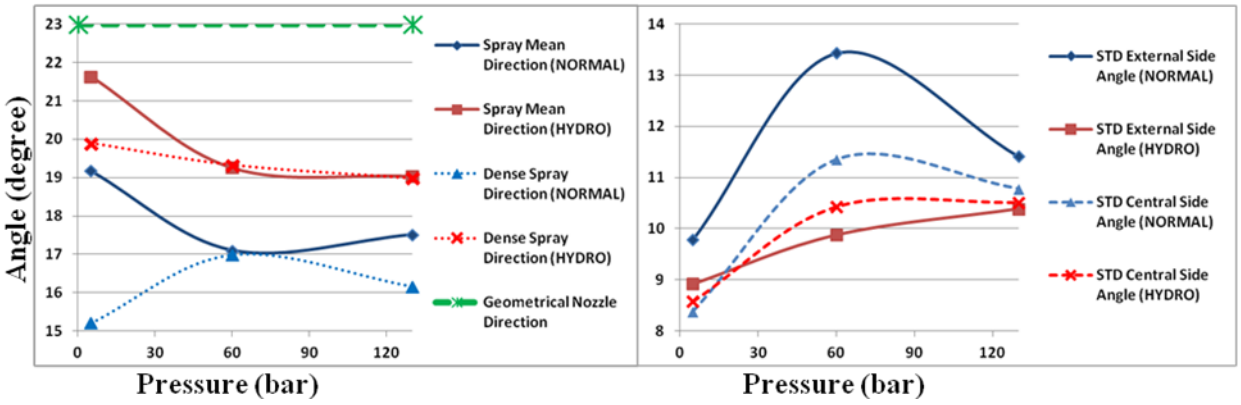


**Figure 3: Comparison of spray mean direction, dense spray mean direction and standard deviation.**

Figure 3 right hand side graph shows the standard deviation on each side of the jet mean direction for both injectors. Results show a similar behaviour for both injectors on the central side with a slightly larger spray in the case of the normal injector especially at 60 bar. At 5 and 130 bar the gap is reduced. But on the external side the gap between injector sprays is large. The normal injector has a much wider spray on the external side than the hydro injector – standard deviation is around 3.5° higher for normal injector spray at 60 bar, and around 1° higher at 5 and 130 bar. This shows that in the case of "normal" sharp nozzle inlet the spray is subject to more flapping, especially on the external side – cavitation side, than the spray discharged by the hydro injector. Cavitation influences the spray width angle and causes a wider one. Ganippa et al. [10] explained that shedding process and collapse of cavities induce transverse motions to the flow which lead immediately to fluctuations in the spray dispersion at the nozzle exit. Bubble collapse energy can also enhance break-up and dispersion [12].

**3- Studies on the dense spray boundary:**

In this section we will focus on the continuous shadow part. The post treatment procedure applied on shot to shot image splits it and separates the few isolated droplets from the rest of the spray in order to analyze its dense core alone. For 5 bar, the dense shadow part is the continuous liquid core. The dense part is filled to obtain a silhouette image – where liquid phase appears in white on a black background [13, 14] – since only the interface of the continuous shadow interests us as it is seen in figure 4 at the bottom to the left. The dense and continuous shadow part is assumed - in our shadowgraphy approach - to be representative of the dense droplet fog of the spray at 60 and 130 bar.

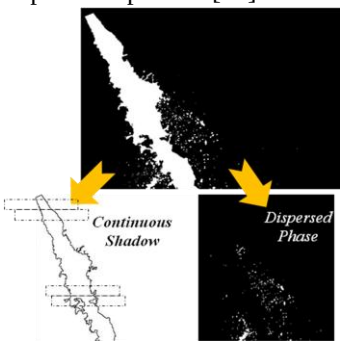


**Figure 4: splitting procedure applied on a 5 bar sample spray image.**

***3.1 Spray wrinkling average:***

To investigate the development of turbulent structures in the spray, the wrinkling of the interface is selected as a relevant parameter. The wrinkling is measured with the interface density S/V, where S is the interface surface and V is the fixed gaseous volume in which our liquid is passing through. In the present investigation, due to the spatial projection, it is substituted by a length density L/S. This ratio is calculated inside a control volume which is a rectangle whose length is constant and height equals the nozzle diameter D. The bottom image to the left (in fig.4) shows the contour of the continuous shadow where the short-dash rectangles schematize the control volume for different iterations throughout distance Z.

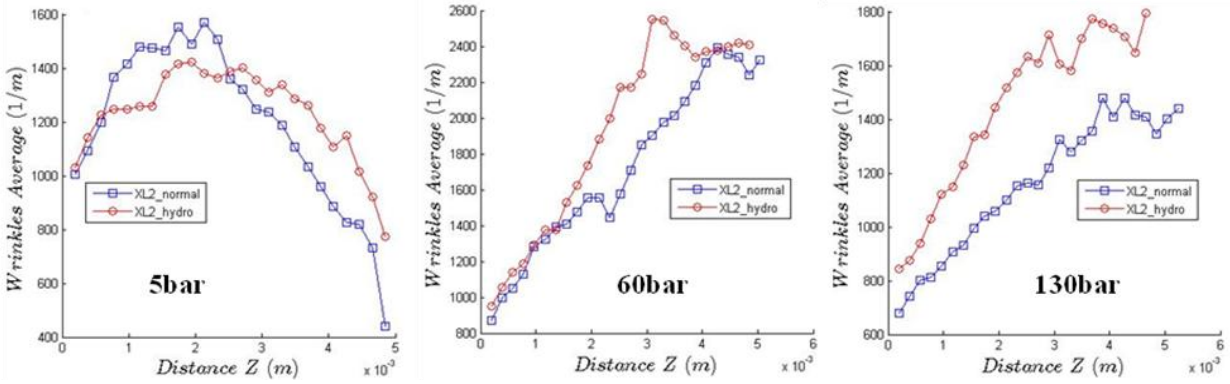


**Figure 5: Comparison of spray wrinkling average throughout distance Z.**

The graphs at 5 and 60 bar (in fig.5) show that the wrinkling generated at 0.82 mm – the first visible on the shadow images – is similar for both designs; contrary to 130 bar where a difference in wrinkling levels is already produced before 0.82 mm.

The wrinkling increases with the distance from the hole, thanks to the instabilities and turbulent structures. For 5 bar, a maximum is reached – the ligaments are broken into separated droplets. The maximum for the normal injector spray case is higher, and once it is reached, values drop quickly. While further downstream (Z > 2.5 mm) the spray issuing from the hydro injector has higher wrinkling values. In average, break-up of the normal injector spray is happening in a small interval at around 2 mm downstream. This interval is wider in the case of the hydro injector spray, which means that its break-up is slightly delayed and its continuous liquid core is bigger in length (see fig.6 the 5 bar graph).

At higher pressures the involved process is different. The break-up length is dramatically reduced – shorter than the initial mask where the flow cannot be visualized. Then, the observed wrinkling is an indication of the spray instability with drop segregation and air engulfment inside the spray. Therefore, the wrinkling of the spray shadow edge is assumed to be an indicator of the spray mixing quality. Comparing the level of the maxima for 60 and 130 bar, the hydro-ground injector has a level of higher wrinkling, especially at 130 bar where it has the better mixing throughout all the distance Z.

### *3.2 Radial distance average:*

Here, the dense spray regions are analyzed in a cylindrical coordinates system (Z,r). The vertical line in the graphs is the direction Z. Figure 6 shows no important differences at 5 bar apart from the dense spray length which is smaller for the normal injector than for the other one as we mentioned before. But at 60 bar the dense spray resulting from the hydro-ground injector looks well centred on the dense spray mean direction throughout the distance Z with a smaller area. In contrary, the normal injector has a diverging left (central) side liquid core. This agrees with the fact that the normal injector always has the smallest angle of dense spray mean direction because its spray is very well dispersed on the external side in comparison to the central side. At 130 bar we note that the dense spray resulting from hydro injector is wider and longer which also means that it is still more compact. This will also be discussed in the section 4 where PDA results are presented.

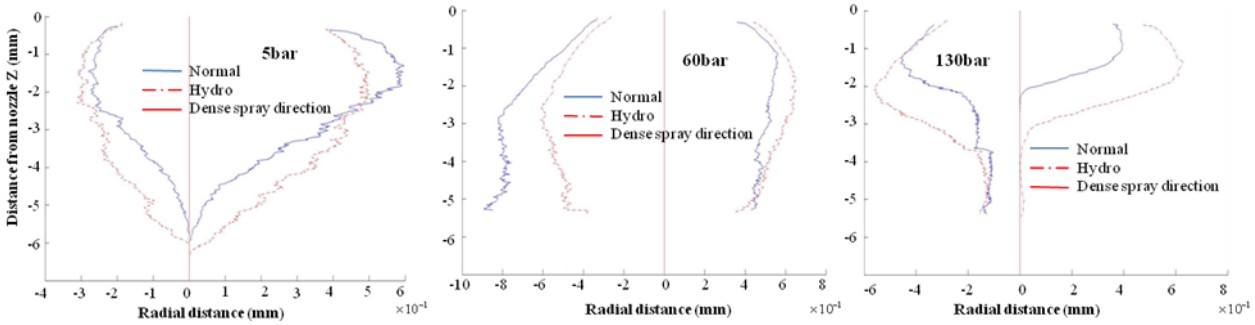


**Figure 6: Comparison of dense spray radial distances (right and left sides throughout Z).**

Results at high pressures lead us to conclude that hydro injector does not disperse the jet as the normal one does at the near field. We can also see that the normal injector creates a dense spray that has a bigger area at the central side than at the external side of the injector; i.e the spray is most dispersed on the cavitation side. The above conclusions support the results presented in section 2.3 which studies the jet mean direction and dense spray direction.

As seen in section 2.3 the normal injector has a wider spray especially on the right side. It also has a smaller dense spray region at this same side as show graphs from section 3.2. Furthermore, the normal injector wrinkling average is less important. The possible explanation is that the flow break-up has already started inside the nozzle. This is due to cavitation which is also coupled with turbulent flow structures in the case of the normal injector. Cavitation is weakened in the hydro-ground injector in comparison to the normal one; therefore break-up is reduced inside the nozzle.

## 4- PDA results:

### *4.1 Velocity results:*

Since cavitation is asymmetric and changes the velocity field of the flow, it is important to compare velocity field of each injector. The hydro grinding also modifies the velocity profile inside the nozzle which leads to higher spray tip speed compared to sharp edge nozzles [15]. Therefore, a downstream position set to 20 mm from the injector tip was chosen for this comparison. Figure 7 compares axial velocity at three different radial positions: 8 mm is almost on the jet mean direction in the middle of the spray, while positions 4 and 10 mm are respectively on the central and external sides of that direction.

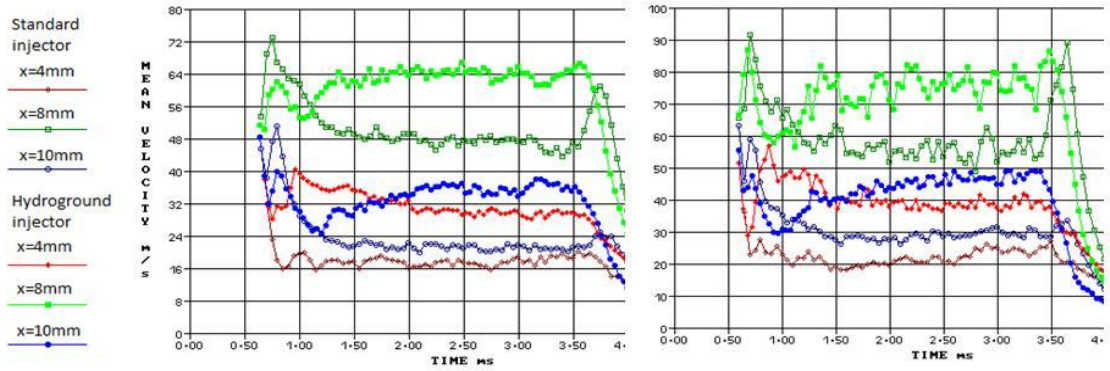


**Figure 7: Axial velocity field at 20mm downstream the injector tip (left side 60bar, right side 130bar).**

The graphs show that the axial velocity in the case of normal injector is reduced in comparison to the hydro-ground one. Results at 60 bar (graph to the left) are similar to results at 130 bar (graph to the right). Velocity is obviously more pronounced at 130 bar than at 60 bar for the all three positions. The difference in spray velocity between the two injector sprays increases at 130 bar as well. Since the spray issuing from the normal injector nozzle is wider and less consistent then it is not surprising that its axial velocity is smaller. The wider a spray spreads, the weaker its axial velocity goes, i.e cavitation appears to be responsible of reducing spray axial velocity through increased spray dispersion that counteracts the internal flow convergence effect. Since this reduction of spray axial velocity is occurring at 20 mm downstream the injector tip, we assume that the over mixing shown in section 3.1 occurs at axial positions very close to the tip (less than 6 mm) but the tendency inverses before this far away (20 mm). For liquid core area wrinkling and atomization, such inversed tendency is visible in the 5 bar graph of figure 6 at 2.5 mm.

### *4.2 Droplet flow angle comparisons:*

All data in this section are taken between 1.5 and 2.5 ms after electronic start of injection, in order to be in quasi-steady conditions. Figure 8, left and right graphs show the droplet flow angle PDFs at 10 mm underneath injector tip for an injection pressure of 60 bar and at 20 mm for 130 bar, respectively. On the Y axis, there is the number of droplets which are situated in the much dispersed area of the near field spray. PDA cannot capture droplets in dense spray areas; this is the reason why droplet numbers are divided by 2 at 130 bar where the near field spray is very dense. While the flow angle values – which are obtained from the axial and radial velocity component vectors of those droplets – are on the X axis. On figure 8 left hand side graph, two radial positions are taken: x = 3 mm – counted droplets are on the left side of the spray, x = 5 mm – they are on the right (external) side. The curves at both radial positions show that the normal injector has wider droplet flow angle PDFs and lower peaks. One can see that the droplets of the dispersed spray area resulting from the hydro injector are much more homogeneous in terms of velocity field while the normal injector's one has more fluctuations. When radial position moves toward the external side, normal injector PDF becomes flat. It is confirmed that cavitation increases the droplet dispersion.

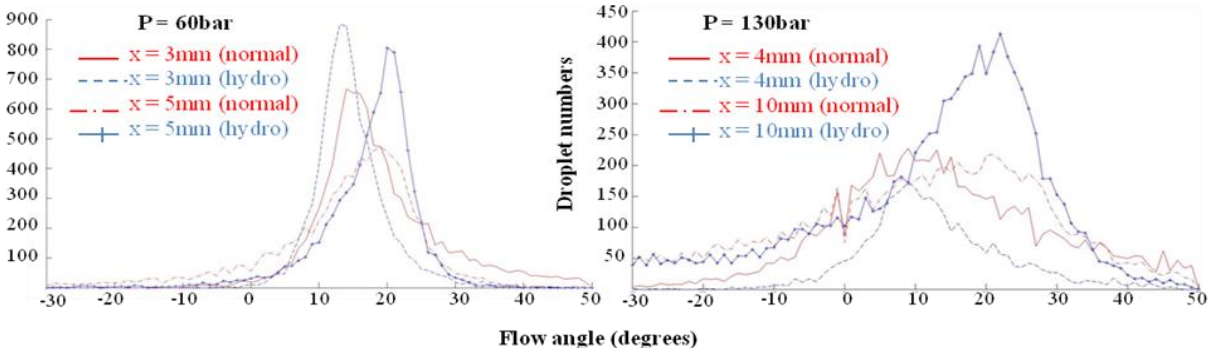


**Figure 8: Comparison between droplet flow angles at both sides of the spray.**

Figure 8 right hand side shows that even when the pressure is increased, sprays still have the same behaviour. At the external side (x = 10 mm), the hydro injector has the highest peak while the normal injector PDF is very flat. Hence, the influence of cavitation on the dispersed spray structure is similar to 60 bar. At the central side of the injector body axis (x = 4 mm) the same effects are observed but less pronounced due to the smaller difference in cavitation on the left side of the nozzle between both injectors.

### *4.3 Droplet sizing:*

In order to investigate the difference in atomization between the two resulting sprays, figure 9 presents 4 graphs with an axial position taken at Z = 50 mm downstream the injector. On the left column, each graph contains two D32 (Sauter Mean Diameter) curves – one for each injector – and two other curves of DV90 (drop diameter such that 90% of total liquid volume is in drops of smaller diameter) – one for each injector as well.

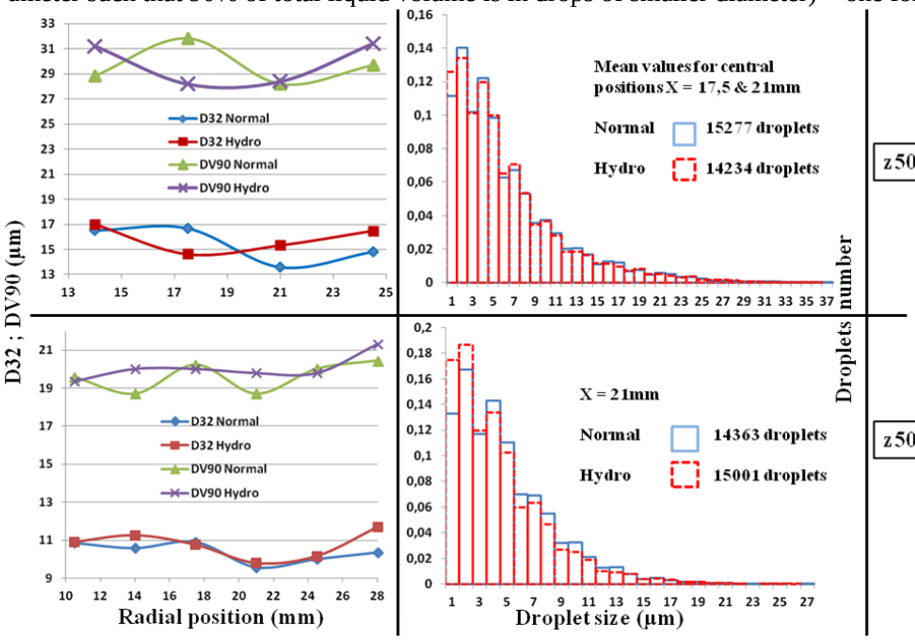


**Figure 9: z50p60 means 60 bar injection pressure and axial position Z = 50 mm (top row) / z50p130 refers to 130 bar injection pressure case (bottom row). D32 and DV90 comparison (left column) / droplet sizing PDF comparison (right column).**

In z50p60 (top graph) case for instance, D32 curves are close with a maximum difference of around 2 µm at the external edge of the spray in favour of the normal injector spray. DV90 values alternate although the gap never goes beyond 3.65 µm. Generally speaking, the difference between the injectors' results in terms of Sauter Mean Diameter and big droplets sizes is very weak, and this is even clearer in z50p130 (bottom graph) case where the gap between D32 is negligible and the gap between DV90 attains not more than 1.3 µm at position 14 mm. In z50p130 case D32 reach not more than 1.3 µm at position 28 mm (external spray edge) in favour of the normal injector. SMD of both injectors are dropping from an average of 15.5 µm in z50p60 case to 10.5 µm in z50p130 case. It means that increasing the injection pressure from 60 to 130 bar decreases the droplets average size about 32% of their initial size. The negligible difference between the two injectors proves that cavitation is not enhancing atomization very much.

The right hand side column in figure 9 shows two droplet sizing PDFs: at the top the injection pressure is 60 bar and at the bottom it is 130 bar. Those PDFs are taken in radial positions at the central core of the jet plume. Only in the case of z50p60 two radial positions were taken and their average data are plotted. PDF graphs show surprising results as both sprays appear to be on a par when it comes to droplet sizing. At 60 bar the normal injector spray has more droplets with low diameter sizes and the gap reaches its maximum value of 237 (droplets) at 2 µm of diameter. Then the gap becomes tighter with the increasing values of droplets diameter. The opposite is happening at 130 bar where hydro injector spray has more droplets with diameters smaller than 4 µm. The gap starts for droplets of 1 µm of diameter at 710 (more droplets for hydro) and is then divided by 2 for 2 µm diameter. Normal injector takes the upper hand starting from a diameter value of 6 µm. Figure 9 shows that both sprays are not easily separable in terms of droplet sizing. As mentioned just before cavitation is not influencing the quality of the final droplets resulting from atomization processes. This is possibly due to the limited level of cavitation of the normal injector, or to the limited effect of the cavitation reduction by hydro-grinding. However, due to the large changes observed in the previous sections, we assume that the equivalent level of droplet size obtained for the two samples is mainly due to the main role of secondary atomization at high Weber and large spray angle as it has been previously shown by Rotondi et al. [16].

## 5- Summary and Conclusions:

In comparison with the normal injector, the hydro injector has only the cavitation structure development weakened thanks to hydro grinding process that rounds the nozzle inlet. Resulting sprays from those two different XL2 nozzle inlet designs were visualized at 5, 60 and 130 bar using shadowgraphy method on a close-up test bench. Images are then analyzed in two different ways as showed sections 2 and 3. To measure spray velocity field and to support the resulting analysis, PDA experiments were conducted for the same cases.

At 5 bar, cavitation enhances the break-up, but wrinkling inverses after 2.5 mm downstream in hydro's favour.

Cavitation changes the atomization of the spray, particularly on the same side where it was developed inside the nozzle. As consequence it can modify the turbulent structures as well as the velocity field of the flow in a way that produce more pronounced transverse fluctuations and a better dispersion of the spray. Appendices A and B show that in the case of the normal injector we can easily distinguish at least two atomization modes. On the other side, the hydro-ground injector shows a consistency in the spray form. The rounded inlet counteracts the cavitation trend and its influence on the atomization.

Finally, the following conclusions about cavitating flow in multi-hole injectors with short L/D were obtained at high pressures and ambient conditions:

- Cavitation on the external side of the nozzle inclines the sloping plume toward the opposite side, especially its dense part.
- Cavitation induces a transverse fluctuation and increases the spray edge flapping mostly on the same side where it was the most developed inside the nozzle. Therefore, asymmetric cavitation causes an asymmetric spray with wider spray angle and smaller dense spray area on the external side.
- Cavitation reduces the mixing of the spray dense area at near field (below 6 mm). In contrary, far away downstream (at least 20 mm at 130 bar) the mixing is found to be inversed.
- Cavitation is responsible of reducing spray axial velocity because of the strong transverse velocity fluctuations.
- Cavitation does not influence the final drop size distribution, but somehow changes the spatial dispersion of the dispersed liquid.

**Acknowledgements:**

This study was supported by MAGIE FUI French project.

**References:**

**[1] N. Leboucher, C. Dumouchel, D. Lisiecki, Y. Wanner,** ICLASS, Heidelberg, Germany, Sept 2012.
**[2] M. M. Khan, J. Helie, A. A. Burluka.** ILASS – Europe, Estoril, Portugal, September 2011.
**[3] J-M. Shi, K. Wenzlawski, J. Helie, H. Nuglisch, J. Cousin. 2010.** ILASS – Europe,Brno, Czech Republic.
**[4] H. Chaves, Ch. Ludwig,** Proc. 20th ILASS – Europe Meeting 2005.
**[5] J. Zhang, Q. Du, Y. Yang,** Tianjin University and Springer-Verlag Berlin Heidelberg 2010.
**[6] C. Badock, R. Wirth, C. Tropea, 1999.** Proc. 15th ILASS – Europe 99, Toulouse.
**[7] G. Wigley, G. Pitcher, H. Nuglisch, J. Helie, N. Ladommatos,** AVL 8th International Symposium on Combustion Diagnostics, Baden-Baden, Germany 2008.
**[8] A. Sou, S. Hosokawa, A. Tomiyama,** International Journal of Heat and Mass Transfer, 2007, *50*, 3575-3582
**[9] R. Miranda, H. Chaves, U. Martin, F. Obermeier,** Proc. ICLASS 2003 Sorrento.
**[10] L.C. Ganippa, G. Bark, S. Andersson, J. Chomiak,** Experiments in Fluids 36 (2004) 627-634.
**[11] L.C. Ganippa, G. Bark, S. Andersson, J. Chomiak,** SAE Paper 2001-01-2008.
**[12] O. J. Soriano Palao, S. Mouvanal,** SAE Paper 2011-28-0120.
**[13] C. Dumouchel, S. Grout 2009,** Int. Jr. of Multiphase Flow.
**[14] S. Grout, J. Cousin, C. Dumouchel,** ICLASS 2006-050 Kyoto Japan.
**[15] S. Kampmann, B. Dittus, P. Mattes, M. Kirner,** SAE Paper 960867, 1996.
**[16] R. Rotondi, J. Hélie, C. Leger, M. Mojtabi, G. Wigley,** ILASS – Europe 2010, Brno, Czech Republic.

**Appendix A: jets at 60 bar**

**Normal injector** **Hydro injector**

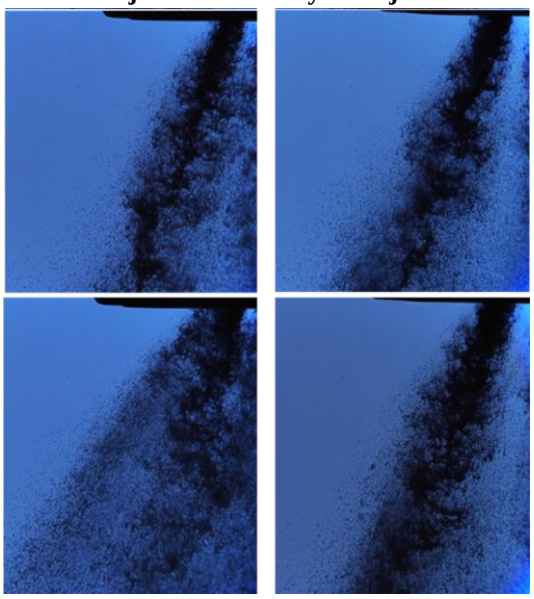

**Appendix B: jets at 130 bar**

**Normal injector** **Hydro injector**